COBEM 2021 26th International Congress of Mechanical Engineering
November 22-26, 2021, Virtual Congress, Brazil

COB-2021-1037
ELBOW MODULE VALIDATION OF A ROBOTIC ORTHOSIS FOR STROKE REHABILITATION

Guilherme de Paula Rúbio
Fernanda Márcia Rodrigues Martins Ferreira
Universidade Federal de Minas Gerais, Graduate Program in Mechanical Engineering, Belo Horizonte, MG, Brazil
Av. Antônio Carlos, 6627 - Pampulha - Belo Horizonte - MG - CEP: 31270-901
guilhermeprubio@gmail.com
nanda_rodrigues06@gmail.com

Rina Mariane Alves Dutra
Universidade Federal de São João del-Rei, Ouro Branco, Centre for Innovation, Research and Teaching in Mechatronics, MG, Brazil
Rododovia: MG 443, km 7 - Ouro Branco - MG- CEP: 36420-000, Brazil
Universidade Federal de Minas Gerais, Graduate Program in Mechanical Engineering, Belo Horizonte, MG, Brazil
Av. Antônio Carlos, 6627 - Pampulha - Belo Horizonte - MG - CEP: 31270-901
rina@ufsj.edu.br

Arthur Mazzini da Mata
Universidade Federal de Minas Gerais, Department of Mechanical Engineering, Belo Horizonte, MG, Brazil
Av. Antônio Carlos, 6627 - Pampulha - Belo Horizonte - MG - CEP 31270-901
arthurmazzini@ufmg.br

João Paulo Fernandes Bonfim
Universidade Federal de Minas Gerais, Department of Electrical Engineering, Belo Horizonte, MG, Brazil
Av. Antônio Carlos, 6627 - Pampulha - Belo Horizonte - MG - CEP 31270-901
jpfb2015@ufmg.br

Claysson Bruno Santos Vimieiro
Universidade Federal de Minas Gerais, Graduate Program in Mechanical Engineering, Belo Horizonte, MG, Brazil
Av. Antônio Carlos, 6627 - Pampulha - Belo Horizonte - MG - CEP 31270-901), and
Pontifícia Universidade Católica de Minas Gerais, Graduate Program in Mechanical Engineering, Belo Horizonte, MG, Brazil
Av. Dom José Gaspar, 500 - Coração Eucarístico - Belo Horizonte - MG - CEP 30535-901
claysson@pucminas.br

Abstract. *Stroke is a common disease that affects countless people around the world, resulting in sequels in the upper limbs. An upper limb robotic orthosis was developed at LabBio to help post stroke people's rehabilitation. In this study was aimed to theoretically and numerically validate its elbow module through kinematics and dynamics models. For this was used Euler vectorial analysis and finite element method, with Mechanical® module of Ansys®, to ensure the correct functioning of the device, effectiveness, structural integrity, and safety before testing on humans. To movement the user's forearm was estimated torque of 4.8 Nm, however the actuator output torque is greater than the estimated torque, presenting a maximum of 12 Nm. Validating the module to clinical tests, the forearm rod has the maximum stress of 24.98 MPa and strain of 0.012%, with a safety factor of 3.8, and the arm structure has maximum stress of 49.72 MPa, and strain of 0.082%, with a safety factor of 1.91, ensuring the safety and capacity of the elbow module in rehabilitation.*

Keywords: *robotic orthosis, elbow joint, theoretically validate, vectorial analysis, structural analysis*

1. INTRODUCTION

The Stroke according to the World Health Organization (WHO) is a sudden interruption of blood flow to brain tissue, due to ischemia or hemorrhage, resulting in the death of brain cells and, consequently, partial loss of neurological function (World Health Organization, 2012). According to the location, amplitude, and severity of the injury, stroke causes a variety of motor, sensory and cognitive deficiencies (Langhorne *et al.*, 2011). Stroke is the main cause of impaired motor functions of the upper limb (O'Donnell *et al.*, 2016). Studies have shown that robotic rehabilitation leads to an

improvement in motor function (Araújo *et al.*, 2011). This is because treatment success is dependent on the intensity and number of repetitions performed in rehabilitation, which are generally less than ideal, when performed manual form by health professionals (Hayward and Brauer, 2015; Stewart *et al.*, 2017), consisting of stimulation of brain plasticity through the passive movement of the affected limb (Langhorne and Legg, 2003; Raffin and Hummel, 2018). The Laboratório de Bioengenharia (LabBio) of the Universidade Federal de Minas Gerais (UFMG), have been developing this type of device, a robotic orthosis for upper limbs to rehabilitate individuals who have suffered a stroke, which also was previously presented at COBEM 2019 (Rúbio *et al.*, 2019). Although, to the use of this device in individuals, it is necessary to validate all the structures' mechanism to ensure safety and effectiveness.

Many robotic orthoses developed have the disadvantage of high weight and volume, such as the prototype called ARMIN-III, an exoskeleton that provides one actuated degree of freedom (DOF) for the elbow joint, and three DOF for the shoulder (Brokaw *et al.*, 2014) and the PNEU-WREX robotic device (Pneumatic Wilmington robotic exoskeleton), capable of generating active force through pneumatic actuators (Reinkensmeyer *et al.*, 2012). Another example is the commercial robotic orthosis, called Myomo e100 (Page *et al.*, 2013), which performs elbow flexion and extension, either actively or passively, and unlike the others apparatus mentioned above, it is a portable orthosis. Although these devices have been used in clinical trials, there exists a lack of theoretical and virtual validation of them before perform bench or functional tests. The device used in this work only validated the hand module (Rúbio *et al.*, 2020), but its elbow module requires a theoretical validation to allow your bench test and clinical trials.

In order to validate this kind of device are several techniques, one form is the numerical analysis and another is using mathematical models of robotic manipulators. One of the validation techniques focuses on prior biomechanical analysis through modeling with CAD (computer-aided design) and later analysis via FEM (Finite Element Method) on the structural parts of the orthoses, this specific work uses generic algorithms for parametric modeling and creation of 3D models for being adapted in CAD and the Voronoi tessellations algorithm (Ricotta *et al.*, 2020). Another validation technique only analyzes the mechanical properties of the materials used in the manufacture of orthosis for the elbow through simulation, the orthosis was subjected to torque and was analyzed through FEM, using SolidWorks (Koundal and Banwait, 2019).

Because of all show, this work aimed a theoretical/virtual validation of the elbow module of an upper limb orthosis, previously developed by the authors, using mathematical models and numerical analysis, in that the correct functioning of the device, effectiveness, structural integrity, and safety for the user was guaranteed. It was expected that using numerical analysis and mathematical models for the elbow module there will be a validation of its design, ensuring the safety of the device during testing with humans and its correct functioning will be guaranteed without requiring more than one bench test.

2. METHODOLOGY

As showed by Rúbio *et al.* (2019), the apparatus analyzed owns two modules, hand modulus and elbow modulus. Due to this, the validation of this device had two main steps, the artificial tendons validation, previously developed in Rúbio *et al.* (2020), and the elbow module validation. This work focuses on presenting how the elbow module was validated to ensure the safety of the user during the clinical trials. In this section, we present the estimate necessary torque to rotate the user's member, the dynamic model of the actuators, the estimated torque of the elbow joint and the structural analysis of the arm structure and the forearm rotation rod.

2.1 Estimated Torque To Rotate The User's Arm

To ensure the safety of the device, the first step needed was the model development of the loads applied in the user's elbow. In that way, it was needed to known how the rehabilitation process could affect the member and the elbow module structure. Post stroke individuals' rehabilitation consists of functional exercise, which aims to promote cerebral plasticity stimulation, i.e, promotes the reorganization and the regeneration of harmed cortical neurons (Langhorne and Legg, 2003; Raffin and Hummel, 2018). During the elbow rehabilitation session, the individual performs intensive flexion and extensions of the member. Analyzing this motion, it was observed that the necessary torque could be determined by the torque to rotate the set of forearm, hand and hand module. In that way, a dynamic model was developed to show the probable torque to move the elbow over time.

Given these movement dynamics to estimate the torque needed, only the mass of the set was considered as a force against the elbow movement. To model this situation was used a lever arm model, with the entire weight of the set concentrated in its Center of Gravity (CG) twisting in relation to the center of the elbow articulation at a constant speed and, consequently, angular acceleration was null. We assume the angular acceleration null, including the initial acceleration, because the motor used (EC16® from Maxxon Motors™) uses a driver ESCON 50/4, which allow an acceleration ramp configurable, and in the initial position the torque produced by the set weight was minimum, because the angle with the lever arm and the weight vector was just of 10°.

The elbow joint maximum and minimum angular positions were considered as the necessary range to performed daily

life activities. According to Neumann (2011), the maximum amplitude of the elbow joint is 5° to 145°, however, for the common activities of daily life, the arch elbow movement is between 30° to 130°. Due to these features, it was defined that the model amplitude movement was between 10° up to 120°, to avoid the maximum extension limits and allows most of the daily activities performed by the user. To determine the elbow position over time was considered, a flexion or extension time of 5 seconds. This time allows the user to perform this movement at a speed equivalent to approximately 11% of the maximum speed that a healthy joint promotes (Valevicius *et al.*, 2019). The choice of this operational range aims to ensure safety and not cause injuries to users. The positions were determined using a time step of 10^{-4} seconds.

With these dynamics considerations presented and following the diagram shows in the Fig. 1, the Eq. (1) was used to estimate the necessary torque over time to move the user's elbow, where the R_g term was the distance between the center of the elbow and the relative CG, P was the weight of the set, θ_0 was the initial position of the elbow ($\pi/18$ [rad]), ω was the constant velocity ($11\pi/90$ [rad/s]) and Δt was the time analyzed.

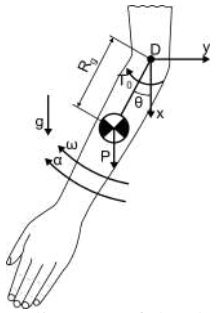

Figure 1: Force diagram of the dynamic model.

$$T_o = P.\,R_g.\sin\left(\theta_0 + \omega\cdot\Delta t\right) \tag{1}$$

In order to determine the weight of the set and your CG location, for the hand and the forearm anthropometric data available in the literature were utilized, whilst for the elbow module the software SolidWorks® was utilized. The forearm and hand mass and CG were determined according to Winter (2009) which says that the hand mass represents 0.6% of the body mass, while the forearm represents 1.6% of the body mass. He also claims that the length of the hand is 10.8% of the individual's total height, while the forearm is 14.6% of the height and the CG location could be obtained through the member length in relation to its proximal location, i.e., the part of the limb most close to the trunk. The hand CG was located in 0.506 times its length and the forearm in 0.430 times its length. Using the MacLeod (2013) data was defined that the average mass of the Brazilian worker was 86 kg and the average height 1.81 m. The last part of the set was the hand module. The mass of the module was directly measured in the prototype, and its CG was determined using a virtual model developed in SolidWorks®, considering its proximal extremity was located at 0.105 m from the elbow joint.

With the data of each part of this set, was determined your relative CG with the reference rotation center as the elbow joint. The Tab. 1 shows the CG location of each component relative to the proximal point of the limb and relative with the elbow joint. Using this, the CG of the set was located at 195.2 mm of the elbow joint, i.e, the lever arm R_g. To find this value, the Eq. 2 was solved using a Matlab® routine, where m_h, m_f and m_{hm} were the mass of the hand, the forearm and the hand module respectively, and x_h, x_f and x_{hm} were the location of the CG relative to the elbow joint center of the hand, the forearm and the hand module respectively.

Table 1: Mass and CG location of the set: forearm, hand and hand module.

Part set	**Mass**	**Length**	**CG Relative to**	
			Proximal Point	**Elbow Joint Center**
Forearm	1.376 kg	0.264 m	0.114 m	0.114 m
Hand	0.516 kg	0.196 m	0.099 m	0.363 m
Hand module	0.618 kg	-	0.131 m	0.237 m

$$R_g = \frac{m_h \cdot x_h + m_f \cdot x_f + m_{hm} \cdot x_{hm}}{m_h + m_f + m_{hm}} \tag{2}$$

2.2 Actuator Dynamic Model

The elbow module actuator consisted of a four bar mechanism, which owned three rotation joins (A, C and D joints) one helical joint (B joint), which is the nut of motor and transmission system set. As shows in the Fig. 2a the link 1 is the

rod what is coupled the motor and the power screw of the transmission system, the link 2 was the nut (B joint) and in its down right extremity is coupled the rotation joint C, the link 4 is the lever arm which is couple with the forearm rod and rotate the user's arm. Finally, the link 1 is the arm structure, where the joint A and D is coupled. More details about the dimensions and statics characteristics were shown in the authors' previous work (Rúbio *et al.*, 2019). In the Fig. 2a, F_m was the input force provided by the motor and transmission system, also previously calculated in the Rúbio *et al.* (2019) work. That mechanism configuration was the basis of the forwards analysis.

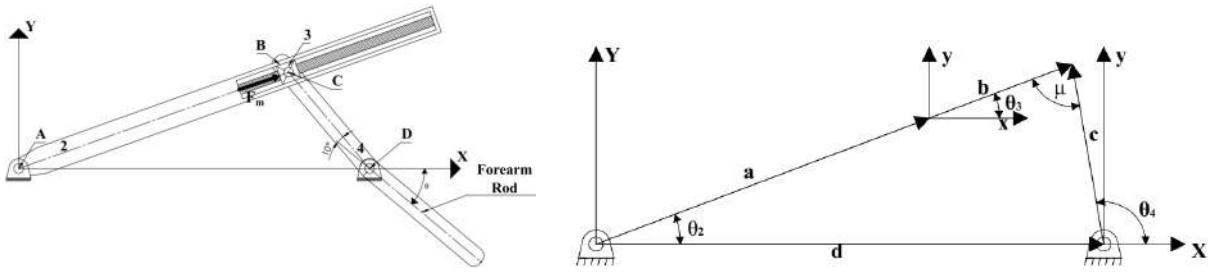

(a) (b)

Figure 2: Model mechanical (a) and vectorial (b) diagram.

Following Euler's identity, a vectorial analysis of the mechanism was performed, using the vectors showed in the Fig 2b. The angle θ_4 was the position reference of the analysis, since this represents the joint was located centrally with the user's elbow. How could be observed in Fig 2a the angle θ_4 was lagged in $10°$ with the forearm rod, which staid coupled with the individual's forearm. Due to this the angle θ_4 varied with same speed of forearm presented in the last section but with the start position of $8\pi/9$ [rad] contrary to the $\pi/18$ [rad] used in the estimated torque equation (Eq. 1). The time step utilized and the maximum and minimum positions of the forearm rod was also the same as those used in the torque estimation.

The dynamic model was developed to determine the actuator temporal output torque. Firstly was determined the positions of the joints A (θ_2), B (b), D (θ_4) as shown in the Eq. 3. As presented in Fig 2b, a was the link 2 length (121.96 mm), b was the helical joint variable length, which was co-linear with a, c was the link 4 lever arm length (65 mm) and d was the distance between the rotating joints A and D (181 mm). In order to find out the speeds of the joint A (ω_2) and B $(\dot{b})$, Eq.4 was used. The joint D speed (ω_4) was constant, with the value of $11.\,\pi/9$ [rad/s]. The accelerations of the joints A (α_2) and B $(\ddot{b})$ were determined using the Eq. 5.

$$\begin{cases} \theta_2(t) = \arccos\left[\frac{(a+b(t))^2 - c^2 + d^2}{2.d.(a+b(t))}\right] \\ b(t) = \sqrt{2.\,c.\,d.\cos(\theta_4(t)) + c^2 + d^2} - a \\ \theta_4(t) = \frac{8.\pi}{9} - \frac{11.\pi}{90}\cdot \Delta t \end{cases} \tag{3}$$

$$\begin{cases} \omega_2(t) = \frac{c.\omega_4.\cos(\theta_2(t) - \theta_4(t))}{a+b(t)} \\ \dot{b}(t) = c.\,\omega_4.\sin(\theta_2(t) - \theta_4(t)) \end{cases} \tag{4}$$

$$\begin{cases} \alpha_2(t) = \frac{c.(\omega_4(t))^2.\sin(\theta_2(t) - \theta_4(t)) - 2.\dot{b}(t).\omega_2(t)}{a+b(t)} \\ \ddot{b}(t) = (a+b(t)).\,(\omega_2(t))^2 - c.\,(\omega_4(t))^2.\cos(\theta_4(t) - \theta_2(t)) \end{cases} \tag{5}$$

With the kinematic of each link proper determined, the dynamics of the actuator system was to find out. Using the free body diagrams presented in Fig. 3 was performed the sum of forces relative of the CG in each link. In Fig. 3a was shown the force between the links 1 and 2 (F_{12}), the force applied by the motor (F_m) and its perpendicular component (F_{23_t}) and the distance of the CG of the link 2 to the joint A (R_{12}), and to the joint B (R_{32}). Besides, the Fig. 3b shows the force between the links 3 and 4 (F_{34}) and the distance between the CG of the link 3 and the joint C (R_{43}). At last, the Fig. 3c demonstrates the interface force in the links 4 and 1 (F_{14}), the output torque (T_o) and the distance of the CG of the link 4 until the joints C (R_{34}) and D (R_{14}). The distances between the joints and the CG of the links and its moments of inertia were measures using virtual models in SolidWorks®as show in Tab 2.

To better comprehension of the forces in the system, the acceleration of each actuator part was derived in two Cartesian vectors centered in the CG and parallel if the global coordinates' system. The Eq. 6 show the new acceleration components

Table 2: Inertial properties of the elbow module actuator mechanism links.

Link	Mass [g]	Moment of inertia $\left[\frac{g}{m^3}\right]$	CG Position [mm]	
			x'	y'
2	160.72	0.65	95.17	0
3	9.24	$5.70.10^{-4}$	-13.11	0
4	101.47	0.77	9.84	141.59

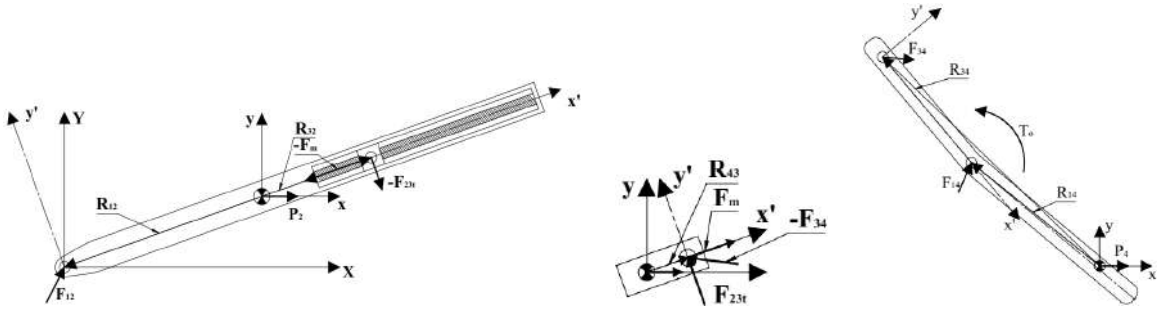

(a) (b) (c)

Figure 3: Free body diagrams of link 2 (a), 3 (b) and 4 (c).

to each link.

$$\begin{cases} A_{G2_x}(t) = -R_{12}.(\alpha_2(t).\sin(\theta_2(t))) + ((\omega_2(t))^2).\cos(\theta_2(t))) \\ A_{G2_y}(t) = R_{12}.(\alpha_2(t).\cos(\theta_2(t)) - ((\omega_2(t))^2).\sin(\theta_2(t))) \\ A_{G3_x}(t) = \begin{array}{l}[-(a+b(t)-R_{43}).(\alpha_2(t).\sin(\theta_2(t)) + ((\omega_2(t))^2).\cos(\theta_2(t)))- \\ -2.\dot{b}(t).\omega_2(t).\sin(\theta_2(t)) + \ddot{b}(t).\cos(\theta_2(t))]\end{array} \\ A_{G3_y}(t) = \begin{array}{l}[(a+b(t)-R_{43}).(\alpha_2(t).\cos(\theta_2(t)) - (\omega_2(t)^2).\sin(\theta_2(t)))+ \\ +2.\dot{b}(t).\omega_2(t).\cos(\theta_2(t)) + \ddot{b}(t).\sin(\theta_2(t))]\end{array} \\ A_{G4_x}(t) = -R_{14}.(\omega_4^2).\cos(\theta_4(t) - 168.93°) \\ A_{G4_y}(t) = -R_{14}.(\omega_4^2).\sin(\theta_4(t) - 168.93°) \end{cases} \tag{6}$$

Finalized the coordinate change of the accelerations, was utilized the Eq. 7 to find out the actuator dynamic forces and its output torque to compare with the estimated torque determined. The I_2 and I_3 variables were the inertia module of links 2 and 3 respectively. A Matlab® routine was used to solve the system of equations.

$$\begin{cases} F_{12_x} - F_{23t_x} = m_2.A_{G2_x}(t) - P_2 + Fm.\cos(\theta_2(t)) \\ F_{12_y} - F_{23t_y} = m_2.A_{G2_y}(t) + Fm.\sin(\theta_2(t)) \\ F_{23t_x} - F_{34_x} = m_3.A_{G3_x}(t) - P_3 + Fm.\cos(\theta_2(t)) \\ F_{23t_y} - F_{34_y} = m_3.A_{G3_y}(t) + Fm.\sin(\theta_2(t)) \\ F_{34_x} + F_{14_x} = m_4.A_{G4_x}(t) - P_4 \\ F_{34_x} + F_{14_x} = m_4.A_{G4_x}(t) \\ -F_{34_x}.R_{34_y} + F_{34_y}.R_{34_x} - F_{14_x}.R_{14_y} + F_{14_y}.R_{14_x} + T_o = 0 \\ F_{23t_x}.\cos(\theta_2(t)) + F_{23t_y}.\sin(\theta_2(t)) = 0 \\ \begin{array}{l}[-F_{12_x}.R_{12_y} + F_{12_y}.R_{12_y}+ \\ +F_{23t_x}.(R_{32_y} - R_{43_y}) + F_{23t_y}.(R_{43_x} - R_{32_x})+ \\ +F_{34_x}.R_{43_y} - F_{34_y}.R_{43_x}]\end{array} \quad = (I_{G2} + I_{G3})\alpha_2(t) \end{cases} \tag{7}$$

2.3 Structural Analysis

After the dynamics analysis, a structural analysis was performed in the two major components of the system, the forearm rod and the arm structure, both made with aluminum alloy 1100 H14 with yield strength of 95 MPa and elongation of 5% (METALTHAGA, 2019). To this validation, a finite elements analysis was done with the Mechanical® module of Ansys®. The two studies followed these steps: virtual modeling, mesh independence test, boundary conditions and post-processing of the results. All parts studied were firstly model in SolidWorks® and after exported to Ansys®. In the realization of the mesh independence test, was performed using three meshes, which in each simulation the number of nodes was duplicated. The boundary conditions of the both study were the critical load condition found with the Eq. 7.The simulations coordinate system was the same shown in the Fig. 3c. The material utilized was the aluminum 1100 H14. The simulations were performed in a computer using Microsoft Windows 10® operational system with 16 Gb of RAM memory and processor Intel® Core™ i7-4790.

To the forearm rod simulation, the load critical point was when the output torque value was 11.99 Nm. In that point, the interface forces between links 1 and 4 (F_{14}) and links 3 and 4 (F_{34}) were 186.49 N and 185.55 N, respectively. At the joint D location a cylindrical support, not presenting radial movement resistance, was defined. All the boundary conditions were shown in the Fig. 4. In order to validate the mesh was used a probe point defined in a chose face as shown in Fig. 4. That probe was defined to assess the maximum von Mises stress. To ensure that the mesh did not interfere in the results, the stress variation in the probe could not vary more than 5% among each mesh.

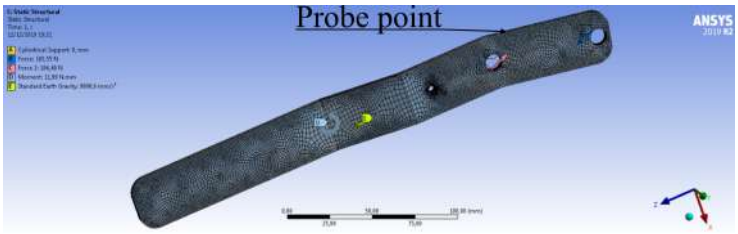

Figure 4: Mesh and boundary conditions of the forearm rod simulation.

The arm structure as a set of plates fixed by bolts, which to simplify the simulations, was omitted. The right side in the Fig. 5 was the link 1 of the mechanism actuator, what responsible to support the actuator loads. The load critic point was the maximum forces between links 1 and 4 (F_{14}), which was 186.55 N. By consequence in the load critic point, the interface force in the links 1 and 2 (F_{12}) which were 183.89 N. Besides, during the elbow flexion the post stroke user presents abnormal synergistic patterns, i.e, when tried the elbow flexion results in shoulder abduction and forearm pronation (Raghavan, 2015). This characteristic leads to a structural torsion of the arm structure. Although the magnitude of that force was unknown, but to predict the structural response to that a binary of forces, with 20 N in magnitude, was applied in the fastening of the joint D, and in its symmetry bolt. Only one support was used, and it was a fixed support applied in the center plate of the structure. All the boundary conditions as shown in the Fig. 5. In its mesh independence test was used a probe point defined in a chose face as shown in Fig. 5. That probe was also defined to assess the maximum von Mises stress. The mesh validation occurred when the stress variation in the probe did not vary more than 5% among each mesh.

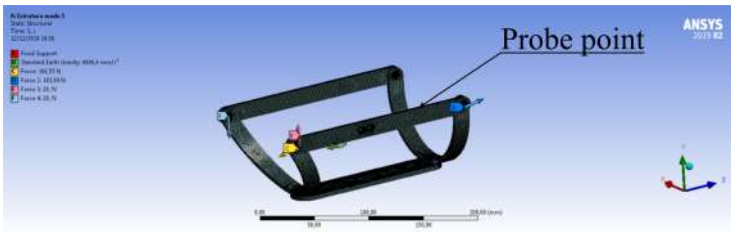

Figure 5: Mesh and boundary conditions of the arm structure simulation.

3. RESULTS

With the estimated torque to rotate the user's forearm using the Eq. 1 and the output dynamic torque calculated by the system of Eq. 7 was possible to compare the two plot as show in Fig 6. As could be seen, the output torque was bigger than the estimated all the time, presenting a maximum value of 12 Nm over a maximum estimated of 4.8 Nm. The higher torque is essentials to ensure the performance of the movement, but, in the way to do not harm the user, with the excessive torque, an electronic safety control was added. With this analysis, the mechanism was validated and could be used in clinical trials.

The device' structural safety was validated through the structural simulations performed. The Tab. 3 shows the mesh independence test. As could be observed, there was almost no variation in the stress measured in the probe point, validating the meshes utilized. The mesh 3 was chosen to the final simulations because of that was solved rapidly, and this component did not have a complex geometry.

Table 3: Mesh independence test to forearm rod simulation.

Mesh	**Maximum von Mises stress [MPa]**	**Number of Nodes**	**Percentage Change**
1	6.91	41,105	0%
2	6.93	81,240	0.30%
3	6.94	167,620	0.15%

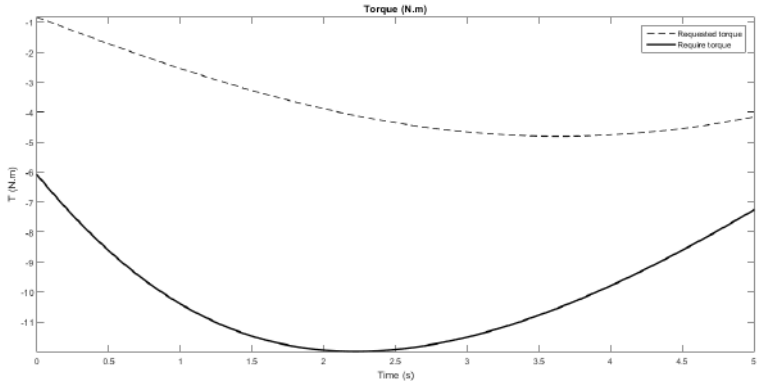

Figure 6: Comparison between the required torque and the torque provided by the actuator.

After the mesh was selected the simulation was solved and the response of the applied loads was presented in Fig. 7. The maximum stress found out was 24.98 MPa located in the joint D hole. The strain present in this point was 0.012%. Due to the low loads calculates, comparing with the material yield strength (95 MPa), with the safety factor of 3.8, the simulation demonstrated the safety of the actuator, ensure that the use in clinical trials do not harm the user.

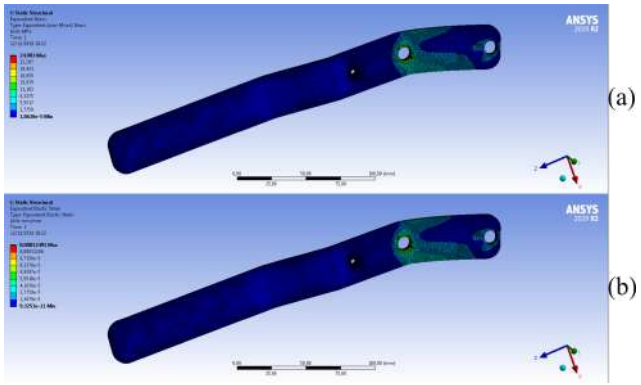

Figure 7: Von Mises stress (a) and strain(b) of the forearm rod.

The simulation results of the arm structure mesh independence test were shown in the Tab. 4. The meshes tested present low variation in the probe point stress value, that confirmed the quality of the mesh. Because of the low variation and the huge number of nodes presents in that simulation, mesh 2 was chosen due to its solve time and its accuracy.

Table 4: Mesh independence test to arm structure simulation.

Mesh	**Maximum von Mises stress [MPa]**	**Number of Nodes**	**Percentage Change**
1	11.96	135,684	0%
2	11.98	248,875	0.17%
3	12.14	503,801	1.34%

At last, the structural evaluation of the arm structure was performed and presented in Fig. 8. As shown, the maximum stress was 49.72 MPa and the maximum strain 0.082%, with a safety factor of 1.91. These values were located in the fastening holes present in the central plate. The left plate almost did not present loads. The low values of stress and strain show this component also safe to use in individuals. This presenting study validates the safety and capacity of the elbow module in rehabilitation users, then enable the next steps, which is to perform the clinical trials.

4. DISCUSSION

Several studies have been measured the active force done by an arm against a rigid surface. Van Harlinger *et al.* (2015) measured the strength of men and women in a large age range (between 20-64 years old) and found a mean value of 26.4 kg for men and 15.4 kg for women. However, there is a gap when the subject is the external force to passively perform flexion or extend the elbow. In other words, there is no literature about the needed force to passively flexion or extend the elbow through an external input performed by equipment measured experimentally. It would be a future work, in order to validate the anthropometric calculus made in this study.

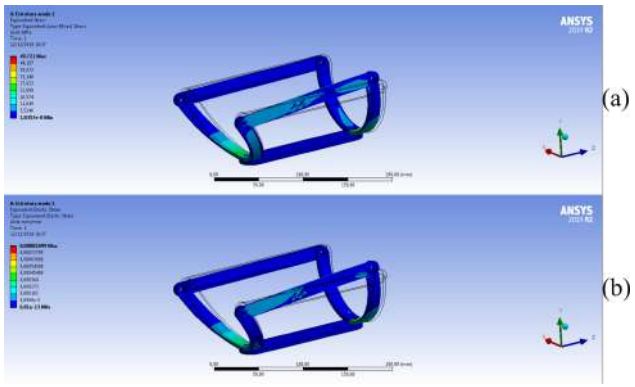

Figure 8: Von Mises stress (a) and strain(b) of the arm structure.

The position analysis of the elbow module in this study was made through Euler's Identity vector analysis. Another common approach to solve this issue is the Jacobian matrices as is shown by Mohammadi *et al.* (2016); Rahman *et al.* (2012). However, using Jacobian matrices can occur robot singularities. It means that the robot has redundant axes, and it results in intolerable torques or forces on the links, loss of stiffness or compliance, and breakdown of control algorithms. The analysis of kinematic singularities is, therefore, an essential step when this approach is used. Nevertheless, Chen *et al.* (2019) proposed a different approach through the POE (product of exponential) formula. The new gravity center (arm wearing the exoskeleton) is not calculated, but it is considered a new coordinate that represents the deviation of the motion center caused by the exoskeleton. The results found by him were similar to the others, validating the approach. Thus, Euler's Identity vector analysis is a powerful methodology once it avoids the problems that can be seen in the literature.

The study was developed considering the movement in two dimensions. It was possible because of the splints which guide the forearm movement. One of the main sequels of the stroke is spasticity, and individuals who have suffered a stroke can develop it. The stress caused by the spasticity was simulated through the binary of forces. Therefore, the splints used in the structure do not allow the unusual movement (wrist and finger flexion) caused by the predominance of hypertonia in the antigravity muscles, that is, the flexors. In a second analysis, a three-dimension analysis of motion would be done like proposed by Mendoza-Vazquez *et al.* (2007). It is relatively easy to compute, because the left part of the Euler Lagrange formulation was computed as if the orthesis were a one link three degree of freedom pendulum, in theory one of the easiest three-dimensional objects to model.

The structure of the elbow was mainly made of Aluminum 1100 H14. Thus, starting with a fixed material and estimating the maximum torque by anthropometric and vectorial methodology, the module was subjected to a structural analysis at ANSYS software, whose results show no irregularities. Nevertheless, Koundal and Banwait (2019) studied the mechanical behavior of several materials using the same software. They considered 20 Nm as torque (higher than the 12 Nm anthropometric estimates) and found the plastic ABS as the best material for this purpose. Therefore, the same methodology involving structural analysis should be applied in several materials. Thus, another material, even lighter than Aluminum, should be used in the elbow structure of the orthosis, which possibilities a new study in material optimization.

In previous studies, it was detected involuntary forearm pronation caused by synergy and spasticity, a stroke sequel (Ferreira *et al.*, 2020). There is no literature that calculates the maximum torque caused by this involuntary pronation, which evidenced the need of studies of these loads in order to use this in the structural optimization of these apparatus, because this effort was essential to be considered in the structural analysis. Due to this, in this study binary of forces on the structure of the elbow module, as shown in Fig. 5, was used to simulate the involuntary pronation torque, and know if the structure supported the efforts caused by this torsion.

Finally, according to this study, the elbow module validation is extremely necessary to help the development of robotic orthoses which are providing an improvement in post stroke rehabilitation. The structure weight and gravity center position need to approximate the real arm to not demand an uncommon effort by the mechanism. In addition, the splints limit the movement in two dimensions, avoiding the actuation of the spasticity. The structural analysis is crucial to evaluate the module's mechanical properties and conclude if the material supports the efforts it will be submitted. Ensuring the device would be able to perform the movements and the angles, it was needed a dynamic analysis. Through it can be calculated the maximum torque of the elbow module.

5. CONCLUSION

Through this study, it is evident the need for validation in robotic orthosis modules. The maximum torque generated was 12 Nm, greater than the estimated flexion of the elbow, which was approximately 4.8 Nm. In addition, the mechanism which uses a bars guided system with force and velocity input by a power screw performs the movements in a satisfactory

way. The structural analysis is important to assure the material will resist the soliciting efforts caused by the module operation. Once the material yield stress is 95 MPa and considering the forearm pronation estimated in 20 N, the maximum von Mises stress found was about 50 MPa. It validates the Aluminum 1100 H14 used, and the simulations are able to validate the critical components of the elbow module. Therefore, it is possible to improve the coupling between the module spindle and the engine. Lastly, the elbow module can be used in rehabilitation protocols to confirm the developed device's ability in rehabilitating post stroke individuals.

6. ACKNOWLEDGEMENTS

The authors would like to thank the Universidade Federal de Minas Gerais, Pontifícia Universidade Católica de Minas Gerais and the Graduate Program in Mechanical Engineering for the support available to carry out this project. We also acknowledge our funders Financiadora de Estudos e Projetos (FINEP), Fundação de Amparo à Pesquisa do Estado de Minas Gerais (FAPEMIG), Coordenação de Aperfeiçoamento de Pessoal de Nível Superior (Capes): finance code 001 and Conselho Nacional de Desenvolvimento Científico e Tecnológico (CNPq) [203345/2019-3].

7. REFERENCES

Araújo, R.C.d., Junior, F.L., Rocha, D.N., Sono, T.S. and Pinotti, M., 2011. "Effects of Intensive Arm Training With an Electromechanical Orthosis in Chronic Stroke Patients: A Preliminary Study". *Archives of Physical Medicine and Rehabilitation*, Vol. 92, No. 11, pp. 1746–1753. ISSN 00039993. doi:10.1016/j.apmr.2011.05.021. URL https://linkinghub.elsevier.com/retrieve/pii/S0003999311003558.

Brokaw, E.B., Nichols, D., Holley, R.J. and Lum, P.S., 2014. "Robotic Therapy Provides a Stimulus for Upper Limb Motor Recovery After Stroke That Is Complementary to and Distinct From Conventional Therapy". *Neurorehabilitation and Neural Repair*, Vol. 28, No. 4, pp. 367–376. ISSN 1545-9683. doi:10.1177/1545968313510974. URL http://journals.sagepub.com/doi/10.1177/1545968313510974.

Chen, W., Li, Z., Cui, X., Zhang, J. and Bai, S., 2019. "Mechanical Design and Kinematic Modeling of a Cable-Driven Arm Exoskeleton Incorporating Inaccurate Human Limb Anthropomorphic Parameters". *Sensors*, Vol. 19, No. 20, p. 4461. ISSN 1424-8220. doi:10.3390/s19204461. URL https://www.mdpi.com/1424-8220/19/20/4461.

Ferreira, F.M.R.M., Rúbio, G., de Avellar, N., Tonelli, L., Brandão, F.H., da Mata, A., Bonfim, J.P., Silva, T., Dutra, R.M., Van Petten, A.M. and Vimieiro, C., 2020. "ROBOTIC ORTHOSIS FOR UPPER LIMB REHABILITATION". In *Proceedings of 1st International Electronic Conference on Actuator Technology: Materials, Devices and Applications*. MDPI, Basel, Switzerland, p. 8519. doi:10.3390/IeCAT2020-08519. URL http://sciforum.net/conference/IeCAT2020/paper/8519.

Hayward, K.S. and Brauer, S.G., 2015. "Dose of arm activity training during acute and subacute rehabilitation post stroke: a systematic review of the literature". *Clinical Rehabilitation*, Vol. 29, No. 12, pp. 1234–1243. ISSN 0269-2155. doi:10.1177/0269215514565395. URL http://journals.sagepub.com/doi/10.1177/0269215514565395.

Koundal, N. and Banwait, S.S., 2019. "Finite Element Analysis of Different Fused Deposit Materials Utilised in Fabrication of Elbow Orthosis". *International Journal of Innovative Technology and Exploring Engineering*, Vol. 8, No. 12, pp. 4847–4850. ISSN 2278-3075. doi:10.35940/ijitee.L3713.1081219. URL https://www.ijitee.org/wp-content/uploads/papers/v8i12/L37131081219.pdf.

Langhorne, P. and Legg, L., 2003. "Evidence behind stroke rehabilitation". *Journal of Neurology, Neurosurgery & Psychiatry*, Vol. 74, No. 90004, pp. 18iv–21. ISSN 0022-3050. doi:10.1136/jnnp.74.suppl_4.iv18. URL http://jnnp.bmj.com/cgi/doi/10.1136/jnnp.74.suppl_4.iv18.

Langhorne, P., Bernhardt, J. and Kwakkel, G., 2011. "Stroke rehabilitation". *The Lancet*, Vol. 377, No. 9778, pp. 1693–1702. ISSN 01406736. doi:10.1016/S0140-6736(11)60325-5. URL https://linkinghub.elsevier.com/retrieve/pii/S0140673611603255.

MacLeod, D., 2013. *THE RULES OF WORK: A Practical Engineering Guide to Ergonomics*. CRC Press, Boca Raton, 2nd edition. ISBN 978-1-4665-6025-3.

Mendoza-Vazquez, R., Escudero-Uribe, A.Z. and Fernandez-Mulia, R., 2007. "Simplified Analytical Dynamic Model for a Parallel Prosthetic Elbow". In *2007 29th Annual International Conference of the IEEE Engineering in Medicine and Biology Society*. IEEE, pp. 3031–3034. ISBN 978-1-4244-0787-3. ISSN 1557-170X. doi:10.1109/IEMBS.2007.4352967. URL http://ieeexplore.ieee.org/document/4352967/.

METALTHAGA, 2019. "Tabela Técnica: Propriedades Mecânicas Ligas de Alumínio Laminadas". URL https://metalthaga.com.br/wp-content/uploads/2017/ 12/5-Propriedades-Mecanicas-Ligas-de-Aluminio-Laminadas.pdf.

Mohammadi, E., Zohoor, H. and Khadem, S., 2016. "Design and prototype of an active assistive exoskeletal robot for rehabilitation of elbow and wrist". *Scientia Iranica*, Vol. 23, No. 3, pp. 998–1005. ISSN 2345-3605. doi:10.24200/sci.2016.3868. URL http://scientiairanica.sharif.edu/article_3868.html.

Neumann, D.A., 2011. *CINESIOLOGIA DO APARELHO MUSCULOESQUELÉTICO*. Elsevier, Rio de Janeiro, 2nd

edition. ISBN 978-85-352-3966-9.

O'Donnell, M.J., Chin, S.L., Rangarajan, S., Xavier, D., Liu, L., Zhang, H., Rao-Melacini, P., Zhang, X., Pais, P., Agapay, S., Lopez-Jaramillo, P., Damasceno, A., Langhorne, P., McQueen, M.J., Rosengren, A., Dehghan, M., Hankey, G.J., Dans, A.L., Elsayed, A., Avezum, A., Mondo, C., Diener, H.C., Ryglewicz, D., Czlonkowska, A., Pogosova, N., Weimar, C., Iqbal, R., Diaz, R., Yusoff, K., Yusufali, A., Oguz, A., Wang, X., Penaherrera, E., Lanas, F., Ogah, O.S., Ogunniyi, A., Iversen, H.K., Malaga, G., Rumboldt, Z., Oveisgharan, S., Al Hussain, F., Magazi, D., Nilanont, Y., Ferguson, J., Pare, G. and Yusuf, S., 2016. "Global and regional effects of potentially modifiable risk factors associated with acute stroke in 32 countries (INTERSTROKE): a case-control study". *The Lancet*, Vol. 388, No. 10046, pp. 761–775. ISSN 01406736. doi:10.1016/S0140-6736(16)30506-2. URL https://linkinghub.elsevier.com/retrieve/pii/S0140673616305062.

Page, S.J., Hill, V. and White, S., 2013. "Portable upper extremity robotics is as efficacious as upper extremity rehabilitative therapy: a randomized controlled pilot trial". *Clinical Rehabilitation*, Vol. 27, No. 6, pp. 494–503. ISSN 0269-2155. doi:10.1177/0269215512464795. URL http://journals.sagepub.com/doi/10.1177/0269215512464795.

Raffin, E. and Hummel, F.C., 2018. "Restoring Motor Functions After Stroke: Multiple Approaches and Opportunities". *The Neuroscientist*, Vol. 24, No. 4, pp. 400–416. ISSN 1073-8584. doi:10.1177/1073858417737486. URL http://journals.sagepub.com/doi/10.1177/1073858417737486.

Raghavan, P., 2015. "Upper Limb Motor Impairment After Stroke". *Physical Medicine and Rehabilitation Clinics of North America*, Vol. 26, No. 4, pp. 599–610. ISSN 10479651. doi:10.1016/j.pmr.2015.06.008. URL https://linkinghub.elsevier.com/retrieve/pii/S1047965115000558.

Rahman, M.H., Saad, M., Kenné, J.P., Archambault, P.S. and Ouimet, T.K., 2012. "Development of a 4DoFs exoskeleton robot for passive arm movement assistance". *International Journal of Mechatronics and Automation*, Vol. 2, No. 1, p. 34. ISSN 2045-1059. doi:10.1504/IJMA.2012.046587. URL http://www.inderscience.com/link.php?id=46587.

Reinkensmeyer, D.J., Wolbrecht, E.T., Chan, V., Chou, C., Cramer, S.C. and Bobrow, J.E., 2012. "Comparison of Three-Dimensional, Assist-as-Needed Robotic Arm/Hand Movement Training Provided with Pneu-WREX to Conventional Tabletop Therapy After Chronic Stroke". *American Journal of Physical Medicine & Rehabilitation*, Vol. 91, No. 11, pp. S232–S241. ISSN 0894-9115. doi:10.1097/PHM.0b013e31826bce79. URL https://journals.lww.com/00002060-201211003-00004.

Ricotta, V., Campbell, R.I., Ingrassia, T. and Nigrelli, V., 2020. "A new design approach for customised medical devices realized by additive manufacturing". *International Journal on Interactive Design and Manufacturing (IJIDeM)*, Vol. 14, No. 4, pp. 1171–1178. ISSN 1955-2513. doi:10.1007/s12008-020-00705-5. URL http://link.springer.com/10.1007/s12008-020-00705-5.

Rúbio, G.d.P., Ferreira, F.M.R.M., Brandão, F.H.d.L., Machado, V.F., Tonelli, L., Kozan, R.F., Santos, C.B. and Vimieiro, 2019. "Design of Actuators Applied to a Upper Limb Orthosis". In *Proceedings of the 25th International Congress of Mechanical Engineering*. ABCM, Uberlândia, MG, Brasil. doi:10.26678/ABCM.COBEM2019.COB2019-0553. URL http://www.sistema.abcm.org.br/articleFiles/download/25287.

Rúbio, G.d.P., Martins Ferreira, F.M.R., Brandão, F.H.d.L., Machado, V.F., Tonelli, L.G., Martins, J.S.R., Kozan, R.F. and Vimieiro, C.B.S., 2020. "Evaluation of Commercial Ropes Applied as Artificial Tendons in Robotic Rehabilitation Orthoses". *Applied Sciences*, Vol. 10, No. 3, p. 920. ISSN 2076-3417. doi:10.3390/app10030920. URL https://www.mdpi.com/2076-3417/10/3/920.

Stewart, C., McCluskey, A., Ada, L. and Kuys, S., 2017. "Structure and feasibility of extra practice during stroke rehabilitation: A systematic scoping review". *Australian Occupational Therapy Journal*, Vol. 64, No. 3, pp. 204–217. ISSN 00450766. doi:10.1111/1440-1630.12351. URL http://doi.wiley.com/10.1111/1440-1630.12351.

Valevicius, A.M., Boser, Q.A., Lavoie, E.B., Chapman, C.S., Pilarski, P.M., Hebert, J.S. and Vette, A.H., 2019. "Characterization of normative angular joint kinematics during two functional upper limb tasks". *Gait & Posture*, Vol. 69, pp. 176–186. ISSN 09666362. doi:10.1016/j.gaitpost.2019.01.037. URL https://linkinghub.elsevier.com/retrieve/pii/S0966636218311779.

Van Harlinger, W., Blalock, L. and Merritt, J.L., 2015. "Upper Limb Strength: Study Providing Normative Data for a Clinical Handheld Dynamometer". *PM&R*, Vol. 7, No. 2, pp. 135–140. ISSN 19341482. doi:10.1016/j.pmrj.2014.09.007. URL http://doi.wiley.com/10.1016/j.pmrj.2014.09.007.

Winter, D.A., 2009. *BIOMECHANICS AND MOTOR CONTROL OF HUMAN MOVEMENT*. John Wiley & Sons, Inc, Waterloo, 4th edition. ISBN 978-0-470-39818-0.

World Health Organization, 2012. "Stroke, cerebrovascular accident." World Health Organization. 27 Set. 2017. URL http://www.who.int/topics/cerebrovascular_accident/en/.

8. RESPONSIBILITY NOTICE

The authors are solely responsible for the printed material included in this paper.